ORIENTING LIGNOCELLULOSIC FIBERS AND PARTICLES BY MEANS OF A MAGNETIC FIELD[1]

Stefan Zauscher[2]
Graduate Research Assistant

and

Philip E. Humphrey[1]
Associate Professor of Forest Products and Materials Science

Department of Forest Products, Oregon State University, Forest Research Laboratory
Corvallis, OR 97331-7402

ABSTRACT

Fiber and particle alignment in composite materials may be used to tailor material and object properties to specific performance requirements. The present research demonstrates that alignment cf ferromagnetically modified slender wood particles in magnetic fields is feasible. Magnetic torque, which causes rotation, increases linearly with the amount of magnetic material on particle surfaces. Below magnetic saturation, magnetic torque increases with increasing strength of the applied field; closer to magnetic saturation, torque becomes less dependent on the applied field strength. Magnetic torque maxima occur at field-to-particle axis angles above 45°. Polarity switches of the applied magnetic field increase particle rotation rates and may counter permanent magnetization, which otherwise tends to impede full particle alignment.

Keywords: Fiber and particle orientation, nickel treatment, magnetic fields, field strength, rotational torque.

INTRODUCTION

The manufacture of particulate or fibrous composite materials often demands tailoring of material properties to specific end-use requirements. This tailoring can be achieved by controlling alignment, dispersion, and volume fraction of particles or fibers (Kelly and Davies 1965; Sutton 1970; Knoblach 1989, 1990; Humphrey 1995). The influence of particle alignment on the performance of wood particle composites was first investigated by von Klauditz et al. (1960), who suggested using electrostatic fields to align particles. This led to the development of electrostatic alignment processes that are currently employed in the manufacture of lignocellulosic (LC) fiber- and wood-composites (Talbott and Stefanakos 1972; Talbott 1974; Suchsland and Woodson 1987; Kawai et al. 1987; Yoshida et al. 1988; Kawai and Sasaki 1989; Yoshida et al. 1989; Pulido et al. 1990; Yoshida et al. 1990; Pulido et al. 1991a, b, c).

Ferromagnetic fibers and nonferromagnetic fibers coated with a ferromagnetic material can be manipulated in a magnetic field (Shine 1982; Hatta and Yamashita 1988; Yamashita et al. 1989). Magnetic fields offer some advantages over electrostatic fields for orientation. First, most fluids are nonmagnetic. Charge polarization effects in the suspending medium, which occur in electric fields, thus do not occur with magnetic fields. Second, high magnetic field strengths can be sustained. In contrast, electric fields collapse when the

---

[1] This is paper 3052 of the Forest Research Laboratory, Oregon State University, Corvallis, OR.

[2] Present address: University of Wisconsin, Materials Science Program % Department of Chemical Engineering, 1415 Engineering Drive, Engineering Hall 4727, Madison, WI 53706.

dielectric strength of the medium between electrodes is surpassed. Third, magnetic fields pose fewer insulation safety problems, and no fire risks due to discharge. Fourth, in the case of magnetically modified LC fibers, interactions with magnetic fields may, for all practical purposes, be assumed to be independent of fiber moisture content (MC). This stands in contrast to electric fields where fiber MC influences the electric torque strongly (Pulido 1991b,c; Zauscher 1993). It is therefore expected that the magnetic torque can be selectively applied to only those fibers that are magnetically modified, and control over alignment can be exercised on a fiber-by-fiber basis.

The objective of this study was to investigate the feasibility of using magnetic fields to exert an aligning torque on magnetically modified wood particles, and to assess the dependence of magnetic torque on field strength, field polarity, and particle treatment.

In the present research, in order to facilitate the understanding of mechanisms underlying particle alignment in magnetic fields, only the alignment of individual, elongated wood particles was considered. However, particle-particle interactions may prove to be very important in practical applications of the approach. Magnetically modified fibers may cause the magnetic field to be locally distorted and, in general, disturbing mechanical interactions due to collisions and entanglement may occur.

THEORY

Wood has an anisotropic diamagnetic susceptibility, which is at a maximum in the direction of the wood fiber length axis. This maximum coincides with the orientation of the crystalline regions of the cellulose chains (Nilakantan 1938). The diamagnetic susceptibility of untreated wood is, however, negligible compared to that of wood having ferromagnetic surface treatments (Zauscher 1992).

To achieve high magnetic torques and short orientation times, it is necessary to coat the wood fibers with strongly magnetic materials.

These ferromagnetic materials have nonlinear magnetic properties and exhibit anisotropy and magnetic hysteresis, which distinguishes them from magnetically linear para- and diamagnetic materials. For the purpose of fiber orientation, ferromagnetic materials with low coercivity (i.e., magnetically soft), low remanent magnetization, high permeability rise factor, and high saturation magnetization are advantageous. A magnetically soft material does not remain strongly permanently magnetized after the external field is removed, and a high permeability rise factor indicates that only a small change in field strength is necessary to achieve a certain increase in magnetization (Siemens AG 1979). Materials with high saturation magnetization offer, in turn, a high magnetic torque at saturation.

The magnetic torque, $T_{(m)}$, on a magnetic particle is a function of the external field, B_y, and the magnetization, M. The magnetization of a ferromagnetic material is generally a nonlinear function of the magnetic field strength to which the material is exposed. The internal field, and the magnetization dependent on it, vary spatially within a magnetic particle according to its shape, its magnetic properties, the particle orientation within the field, and the applied field strength. Except for uniformly magnetized ellipsoids and their degenerate cases, a particle's magnetization vector M is difficult to evaluate (Joseph and Schlömann 1965).

Let us consider uniformly magnetized prolate ellipsoids made from linear magnetic materials that are rotating about one principal axis in an applied field which does not cause saturation. In such a case, magnetic torque is proportional to the square of the applied field strength, to body volume, and to the product of $sin(\alpha)cos(\alpha)$ where α is the angle between the body length axis and the field lines (Stratton 1941; Shine 1982). Magnetic torque increases with increasing aspect ratio and is maximized when α equals 45°. This behavior is analogous to that of a dielectric ellipsoid immersed in an electric field (Okagawa et al. 1974; Okagawa and Mason 1974). Because

magnetic materials have a finite permeability, there exists a limiting particle aspect ratio beyond which the magnetic torque no longer increases (Shine 1982). This stands in contrast to hydrodynamic torque, which always increases with increasing aspect ratio.

At field strengths above those required for saturation, magnetic torque is proportional to the square of the saturation magnetization, and its maximum value is independent of the strength of the applied field. The magnitude of the magnetic torque remains constant as long as saturation is maintained; with decreasing field strengths, however, the angular location at which the maximum occurs shifts towards larger angles.

Magnetic torque on magnetically nonlinear materials must be analyzed numerically. Magnetic torque is proportional to the square of the applied magnetic field strength only for very low applied fields (i.e., in the linear "toe" region of the magnetization curve). If the magnetization level is below saturation, an increase in magnetic field strength yields higher magnetic torques at all particle orientation angles (Shine 1982). However, the dependence of magnetic torque on applied field strengh is not easily assessed since it is intimately related to the particular magnetization behavior of the magnetic material. At field strengths approaching those necessary for saturation, magnetic torque becomes increasingly less dependent on the applied field strength.

The theory for magnetic torque on prolate ellipsoids holds also for slender, uniformly magnetized cylinders having equal aspect ratio and volume (Shine 1982) and is qualitatively true for any slender symmetric magnetized particle. In the case of magnetically heterogeneous bodies, the situation is more complicated because each magnetized particle sets up a magnetic field of its own and is also influenced by the fields of all the other particles.

The equation of motion for a particle subjected to several body and surface forces is based on conservation of linear and angular momentum. Assuming negligible particle inertia, the magnetic torque, $T_{(m)}$, is equal to, and

counteracted by, the hydrodynamic torque, $T(h)$, (Eq. 1).

$$T_{(m)} = -T_{(h)} \qquad (1)$$

With the quasistatic form of the creeping motion equations, the hydrodynamic torque on a particle, and thus also the magnetic torque, can be shown to be directly proportional to fluid viscosity, the particle's angular velocity and to a characteristic shape constant (Brenner 1963; Happel and Brenner 1965; Kim and Karrila 1991).

Analogous to the center of mass in rigid body dynamics, there exists in fluid dynamics a center of hydrodynamic resistance (Brenner 1963; Kim and Karrila 1991), where rotational and translational motion are decoupled. In the case of a homogeneous and geometrically orthotropic body, the centers of hydrodynamic resistance, buoyancy, and mass coincide at the geometric center of the body.

For experimental purposes, a particle is ideally in a neutrally buoyant state and does not translate. But even if such motion occurs, a translational motion along an axis of principal resistance does not impart additional torque on the particle (Brenner 1963; Kim and Karrila 1991). The hydrodynamic torque exerted on the fluid by a particle rotating about one of its axes of principal resistance (i. e. about its center of hydrodynamic resistance) is given by (Eq. 2),

$$T_{(h)} = -\eta c \cdot \omega \qquad (2)$$

where η is the constant fluid viscosity, ω is the particle's angular velocity, and c is the symmetric rotational resistance tensor, which is solely dependent on particle geometry. The components of this tensor are analytically solvable for an ellipsoid and its degenerate cases (Jeffery 1922; Kim and Karrila 1991) but must be determined empirically for almost all other shapes. The magnetic torque is then

$$T_{(m)} = \eta c \cdot \omega \qquad (3)$$

or in component notation,

$$T_{(m)i} = \eta^{C}_{ij}\omega; \qquad\qquad (4)$$

where $i,j = 1,2,3$.

The specific magnetic torque (SMT), $T^s_{(m)}$, on a particle rotating about its ith principal axis (Eq. 5) can be obtained by expansion of (Eq. 4) with the additional constraint of $i = j$

$$T^s_{(m)i} = \frac{T_{(m)i}}{C_{ii}} = \eta\omega_i \qquad\qquad (5)$$

The SMT is therefore solely a function of fluid viscosity and the particle's angular velocity while it is rotating in a plane of principal hydrodynamic resistance, and both variables can be determined by experiment. The SMT is useful in comparing the magnetic torque on particles having identical geometries and consequent hydrodynamic behavior, without knowing their particular hydrodynamic resistance.

METHODOLOGY

Preparation of magnetic particles

For this research small, slender, precisely cut strips of aspen (*Populus* spp.), having the shape of a rectangular parallelepiped (average dimensions: 12.9 × 0.8 × 0.5 mm; average MC: 8.3%) were used. This shape was chosen to approximate LC fibers. In a preliminary attempt to render the wood particles magnetic, nickel was deposited onto their surface by an electroless process (Schlesinger 1974; Nagasawa et al. 1990, 1991, 1992). This method proved unsatisfactory, however, because the deposit had inferior magnetic properties compared to elementary nickel (Schwartz and Mallory 1976; Zauscher 1992). Furthermore, lumen loading (Green et al. 1982; Ricard and Marchessault 1990; Rioux et al. 1992) requires fiber beating, which was not possible in this study. Ultimately, a nickel powder/acrylic binder suspension (Electrodag 440®; 59% nickel [w/w]) was deposited onto the wood particle surfaces in the form of a fine mist. The fiber particles were fluidized using an air stream during the spray operation in order to obtain near-uniform surface treatment and to

avoid particle agglomeration. Treatment batches with nine different target loading levels (plus untreated control samples) were prepared by varying spray time. From these treatment batches thirty-six particles were selected on the basis of optically inferred uniformity of coating and target dimension to within ±0.03 mm.

To evaluate average magnetic properties of the coated particles, mass susceptibility (with a Bartington M.S.2. susceptometer; sensitivity 2.5 × 10⁻⁶) and isothermal remanence magnetization (with a Schoenstedt Digital Spinner Magnetometer, Mod. DSM 1; accuracy ±1%) were measured as functions of applied field strength. They were also measured after demagnetization. The functional dependency between remanence magnetization and the applied field strength reflects that between magnetization and applied field strength. The alternating field required to decrease saturation remanence by 50% is called the medium destructive field; its magnitude is a good indicator for the coercivity of the nickel coating.

Particle rotation experiments

The assumptions made for this study of magnetic torque are summarized in Table 1. To produce the required homogeneous, uniform, and stable magnetic field, an electromagnet (field stability better than 10 ppm; field inhomogeneity smaller than 0.5%) and a matching power supply were designed and constructed (Zauscher 1992). Magnetic field strength was measured with a Hall effect sensor (LDJ HR-70-CP). To determine particle angular velocity during rotation, the particle angle relative to the magnetic field lines was measured as a function of time. Video filming (NIKON 8 mm Cam-Corder, VN-700) of particle rotation proved to be a nonintrusive way to obtain the time-angle information. A stopwatch display (resolution: 1/100 s) was filmed with the rotating particle to obtain the time progression from one video frame to the next. The use of standard video equipment imposed a time-resolution limit of ±1/60 s on the cap-

TABLE 1. *Assumptions made in studying magnetic torque.*

1) Particles are rigid bodies. Centers of gravity, buoyancy, and hydrodynamic stress coincide at the particle's geometric center.
2) Particle inertia is negligible.
3) Particles of identical shape and size exhibit identical hydrodynamic behavior.
4) Particles rotate about one of their axes of principal resistance.
5) The applied magnetic field is stable, uniform, and parallel over the volume in which rotation takes place.
6) Particles are not hysteretic and initially are not magnetized.
7) Magnetic material is uniformly distributed over the particle surfaces.
8) The magnetization adjusts itself instantaneously to its equilibrium value.
9) The suspending fluid is Newtonian.
10) The undisturbed fluid is stagnant and unbounded.
11) Fluid inertia and Brownian motion are negligible.

FIG. 1. Schematic representation of the experimental set-up for particle rotation.

tured events. Figure 1 shows a schematic view of the experimental setup; it is shown photographically in Fig. 2.

Silicone fluids (DOW series 200®) with viscosities between 20×10^{-3} Pa-s and 120×10^{-3} Pa-s were used for nonwetting suspension. Within rheometer accuracy (Brookfield LVTD with small sample adapter SC4-18/13R), differences in the measured viscosities at shear rates comparable to those found in the experiments could not be attributed to non-Newtonian behavior. There was a nearly linear relationship between fluid viscosity and temperature in the range between 20°C and 30°C; regression equations made it possible to correct fluid viscosity for temperature. Temperature was measured with a thermistor probe (YSI 44204) achieving a temperature resolution of ±0.03°C.

Particle rotation was filmed after the sample container was positioned in the field such that the particle approached an unstable equilibrium position ($\alpha \approx 90°$). Angle-time data pairs were obtained from about 30 video images by repeatedly measuring the angle α formed by the particle length axis and a reference line
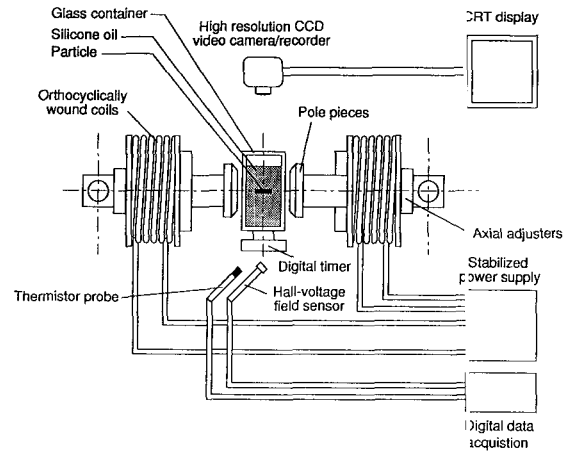
parallel to the magnetic field lines. Angle measurements have an accuracy of ±0.3°.

The data thus recorded yielded a characteristic sigmoidal curve that was approximated numerically by a least-squares fit; differentiation with respect to time generated a function representing the angular velocity (Fig. 3). In order to compare SMT data from different experimental runs, fluid viscosity for each run was corrected for temperature and scaled to an arbitrarily chosen reference viscosity of 50×10^{-3} Pa-s. The particle angular velocities for a given experimental run were then multiplied by the scaling factor and the reference viscosity to yield the SMT. The maximum SMT was
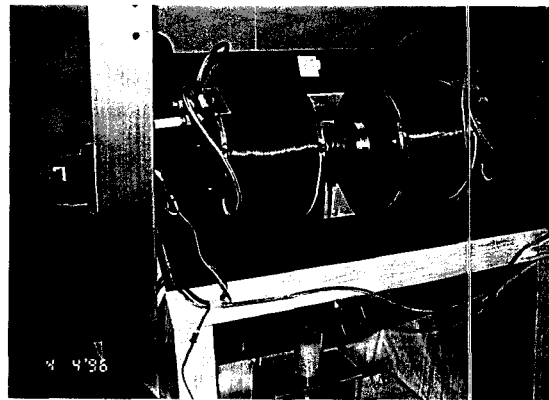

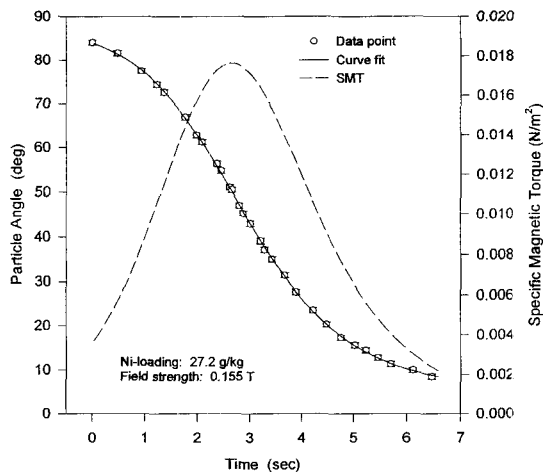FIG. 2. Electromagnet with sample container in position.

FIG. 3. Angular displacement versus time; numerical fit to typical data points and derivative expressed in the form of specific magnetic torque.

used as a characteristic value in the analysis of experimental results.

RESULTS AND DISCUSSION

Magnetic surface treatment

Elemental maps for nickel on particle surfaces indicate a rather uniform surface coverage (Fig. 4). Diameters of the deposits ranged from 70 μm to smaller than 2 μm (measured from micrographs). Variability of up to $\pm20\%$ among the SMT maxima for particles of one treatment batch suggested that nickel content on particles within each of the nine batches varied considerably. Average nickel concentrations among the batches ranged between 5.3 g/kg and 49.7 g/kg (oven-dry particle mass). Both mass susceptibility (Fig. 5a) and saturation isothermal remanence magnetization (Fig. 5b) varied linearly with nickel concentration.

A medium destructive field of 9.5 mT (about 7,600 A/m) indicated that the nickel coating can not be considered magnetically soft; a comparable value exists, for example, for magnetically semi-hard Cr-Co-Fe alloys. Remanence and coercivity values may be expected to differ from values found for pure nickel in a homogeneous sample. Coercivity increases with the particle size in the nickel
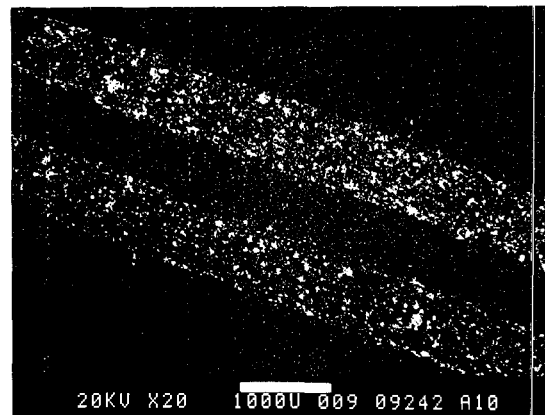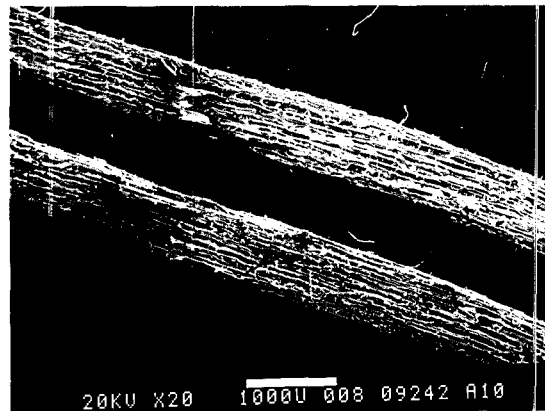

FIG 4. Typical treated particle surface and corresponding element map for nickel on the particle surface (11.6 g/kg nickel, 20×)

coating (typically 2–3 μm), and impurities in the nickel coating may be expected to hinder domain wall movement, which, in turn, increases coercivity (Brown 1962). Particle magnetization behavior (Fig. 6) appears to be independent of nickel concentration on particle surfaces. Over 90% of bulk magnetic saturation was reached at a field strength of 0.1 T (Fig. 6).

The basic nature of particle rotation

A Reynolds number of the order of 2 × 10⁻³, the maximum from all of the experimental runs, supported the assumption of negligible particle inertia. Variability among replicate

runs, inferred from differences in the SMT maxima, ranged from 1% to 3%, and increased with increasing rotation times. Low nickel-loading levels and low field strengths increase rotation times; this, in turn, increases the possibility of particle misalignment (out of the rotation plane) and consequent changes in hydrodynamic resistance.

With a decrease in container diameter, wall effects decreased the angular velocity of a rotating particle. A container with an inside diameter of 23.9 mm was a compromise between errors due to disturbing wall effects and the loss of field homogeneity and strength associated with increasing pole piece separation. Positioning a particle off center was an important source of experimental error. It was estimated that a 1-mm offset reduced the SMT by about 1.7%.

Figure 7a shows three pairs of unscaled but fitted data curves (angular displacement vs. time) for three different fluid viscosities. The curves coincide nearly exactly (Fig. 7b) after the viscosities are scaled to a common value of 50×10^{-3} Pa-s (done by dividing the rotation time of each data curve by the respective viscosity scaling factor). This result supports the assumption that particle rotation scales linearly with both viscosity and angular velocity. Slope differences in the curves below angles of 30° are believed to originate from permanent particle magnetization that occurred during rotation in the magnetic field. To destroy remanence magnetization, each particle was, from then on, demagnetized in an alternating magnetic field (0.14 T peak) of decreasing amplitude prior to further experimental runs.

Dependence of SMT on nickel treatment

The SMT maximum increased linearly with increasing nickel loading (Fig. 8). Mass susceptibility was also linearly dependent on nickel concentration, indicating that the former can be used to predict magnetic torque.

Dependence of SMT on field strength

Experimentation was restricted to magnetic field strengths ranging from 0.07 T to 0.16 T.
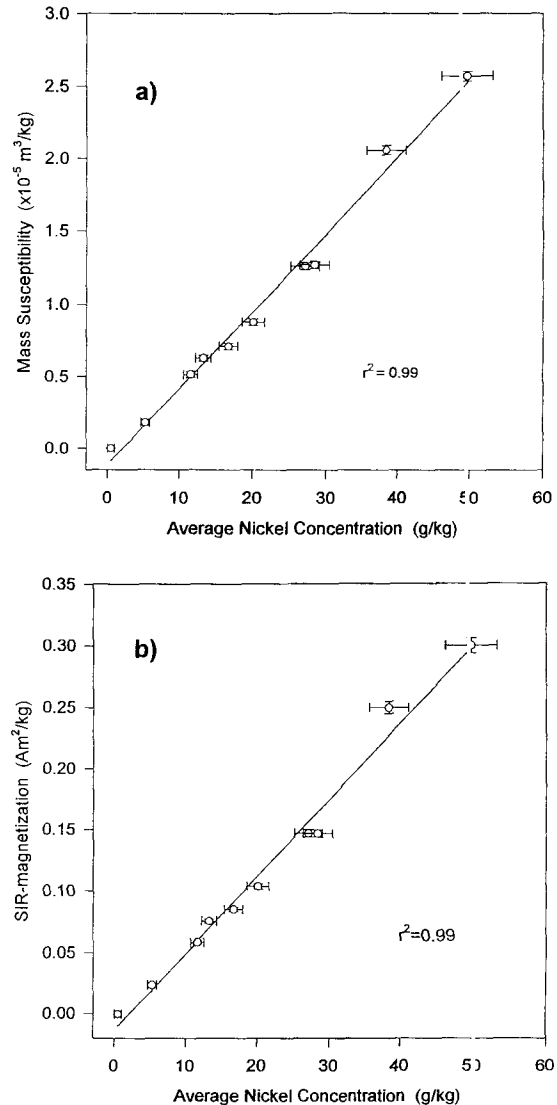

Fig. 5.   a) Mass susceptibility and b) saturation isothermal remanence magnetization as a function of average nickel concentration on the particles. There were nine treatment levels plus an untreated control. Each data point is the average of four samples.

Above 0.16 T, the available magnetic system could not maintain sufficiently stable and uniform fields. Low field strengths caused long rotation times, and disturbing translational particle motion began at fields below 0.07 T. Normalized SMT maxima as a function of applied field strength are compared in Fig. 9 for
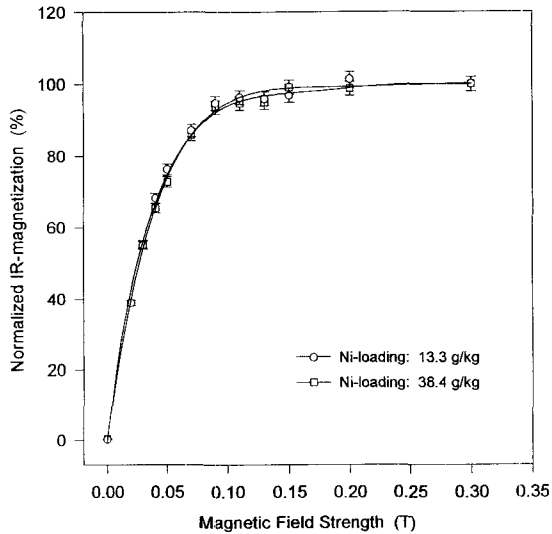
FIG. 6. Normalized isothermal remanence magnetization for two nickel concentrations as a function of magnetic field strength.

a low and a high nickel-loading level. The data suggest an inflection of the SMT maxima at about 0.11 T and a tendency to level off thereafter. This tendency is to be expected, since at field strengths approaching those necessary for saturation, magnetic torque becomes increasingly less dependent on the applied field strength (Shine 1982). It was anticipated that the approach to a limiting SMT value would be more pronounced than was found, since, as shown earlier, over 90% of bulk magnetization is reached at about 0.1 T. The gentler approach suggests that in order to reach a given level of magnetization, larger applied field strengths are required for individual, magnetically coated particles than for the same material in bulk.

A power-law fit to the SMT maxima at fields below the inflection in the data (i.e., fields in the range from 0.00 T to 0.11 T) yielded a higher than quadratic dependence of SMT on applied field strength ($T_{(m)} \propto B_0^{2.56}$). This type of behavior is consistent with that of nonlinear magnetic materials above their linear magnetization region—which usually involves only very low applied magnetic field strengths—but below their magnetic saturation (Shine 1982).
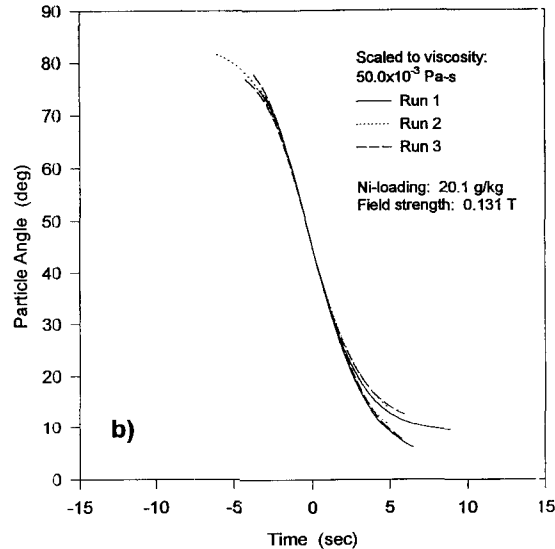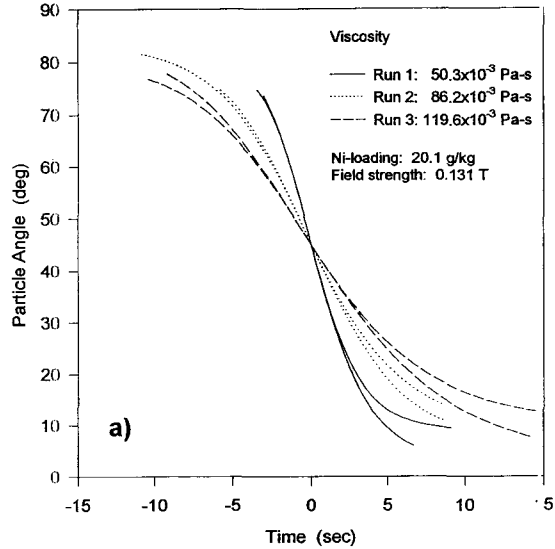

FIG. 7. a) Fitted angular displacement versus time for three different fluid viscosities; b) fitted angular displacement versus time for the viscosities shown in a), scaled to a common viscosity of 50 × 10⁻³ Pa-s.

The SMT and its angular position as a function of applied field strength were obtained numerically from fitted data curves for a range of applied magnetic field strengths (Fig. 10). These show that specific magnetic torque increases quickly with increasing particle alignment to reach a maximum at angles above 45°.
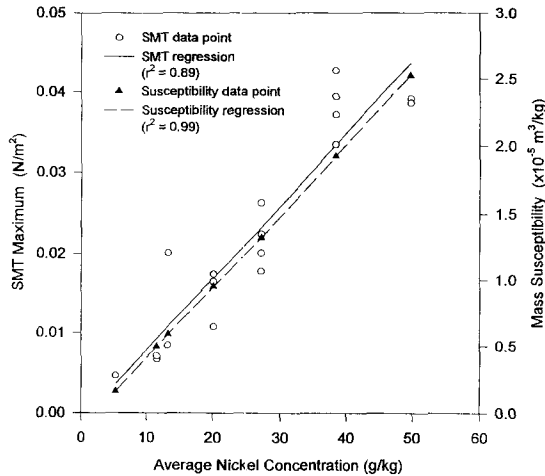
Fig. 8. Dependence of the maximum specific magnetic torque and mass susceptibility on average nickel concentration on particle surfaces.

Fig. 9. Normalized specific magnetic torque maxima for two nickel concentrations as a function of applied magnetic field strength.

Shine (1982) reports that the curvature of the magnetization plot determines the angular location of the magnetic torque maximum. A convex magnetization curve indicates that the torque maximum will be shifted towards larger angles, whereas a concave curve indicates a shift towards smaller angles. An analogous relationship exists between the SMT maxima as a function of applied field strength and the angular location of the these maxima in our experiments. The SMT curves terminate at particle orientation angles between 3° and 20°. This behavior, indicating that full alignment is not reached, appears to be more prominent at low applied field strengths. Reasons for this behavior may have been the consequence of insufficient alignment times (experimental limitation) and unfavorably directed remanent magnetization of the particle surface coating (see discussion below).

Changing field polarity

Experiments were primarily conducted with constant magnetic fields. However, a polarity switch of the applied magnetic field increased magnetic torque and, as shown in Fig. 11, reduced particle alignment times. Polarity switches are most effective at particle align-
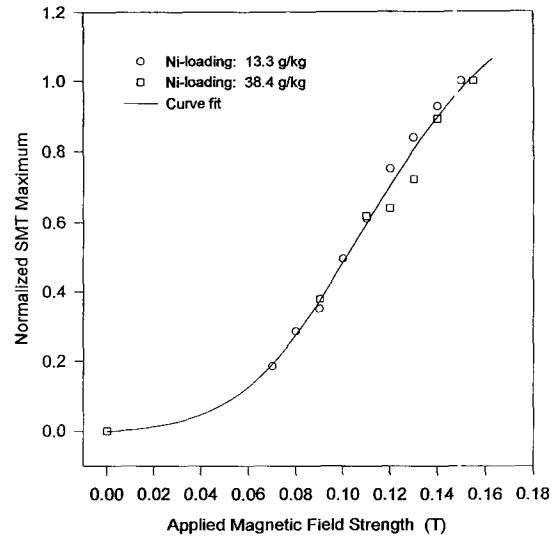
ment angles below 45°. The Hall voltage—indicating magnetic field strength—was monitored with an oscilloscope during field switches and did not detect surges in the magnetic field. It may therefore be concluded that the state of magnetization of the magnetic surface treatment was profoundly changed during a
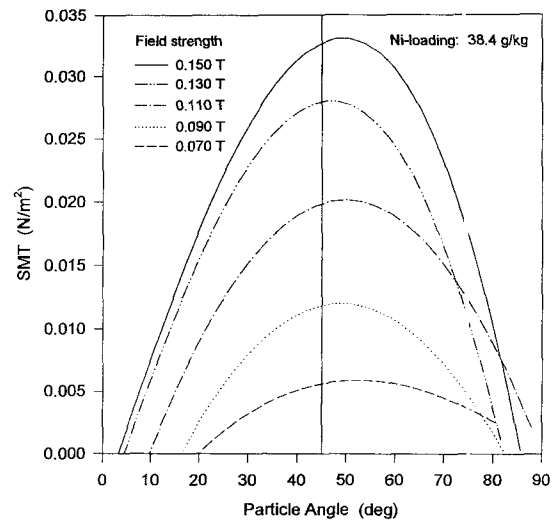

Fig. 10. Specific magnetic torque as a function of angular displacement for a range of magnetic field strengths.
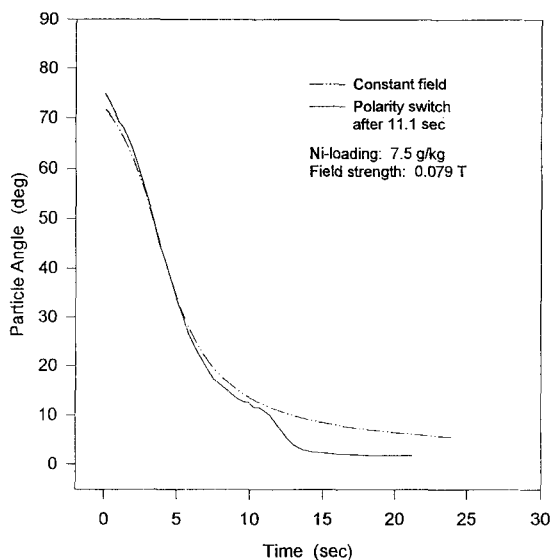
FIG. 11. Angular displacement versus time for two experiments using the same particle: one in which the field was held constant and one in which the field polarity was switched.

polarity switch. The above phenomenon may be a consequence of a mechanism that destroys unfavorably directed remanent magnetization that would otherwise prevent full alignment. The increasing effectiveness of polarity switches with decreasing alignment angles may be explained in terms of magnetic shape anisotropy. The internal magnetic field governing magnetization increases with decreasing demagnetization fields—set up in the magnetic coating due to the shape of the wood particle. These, in turn, become smaller with greater alignment between particle length axis and the magnetic field lines. Remagnetization times are considered negligable compared with possible particle rotation times.

It was energetically advantageous for a particle to rest in a partially aligned equilibrium position after rotation in the magnetic field. Alignment may depend on a particle's magnetic history and may be the consequence of unfavorably oriented permanent magnetization attained during rotation in the field. This hypothesis seems justified when the high coercivity of the magnetic particle coating is considered. As described previously, experiments performed without prior particle demagnetization revealed discrepancies due to permanent magnetization. This applied to alignment angles below 30°. The SMT maxima, which occurred at angles larger than 45°, were not perceptibly influenced.

CONCLUSIONS

Alignment of LC particles under the influence of magnetic fields is feasible if the particles are magnetically modified. Applied fields interact with deposited magnetic material only, and fiber moisture content is therefore not a significant factor. An experimental method developed for the present research enabled study of the magnetic torque on a single particle as a function of treatment level, field strength and field polarity. Repeatability error for this method was about ±2%.

Magnetic torque increases linearly with magnetic fiber loading levels, and susceptibility measurements can be used to predict magnetic torque. This finding may be of considerable practical importance because susceptibility measurements are easily performed. The dependence of the magnetic torque on particle shape can be determined with the present experimental method if the components of the hydrodynamic resistance matrix for that shape are known. Analytically derived predictions for the magnetic torque on magnetically homogeneous slender particles were qualitatively confirmed. At fields below magnetic saturation, but above the linear magnetization region, the magnetic torque rises initially with a higher than quadratic power ($T^s_{(m)} \propto B_0^{2.56}$) of the applied field strength and tapers off at field strengths closer to saturation. The angular maxima of the magnetic torque occurred in all cases above 45°, in agreement with empirical and theoretical predictions. The use of alternating magnetic fields may have great practical importance since shorter rotation times, higher torques, and better particle alignment are achievable. However, the inductance of the

magnet windings may impose a limit on frequency.

The successful orientation of LC particles in a viscous fluid further suggests that orientation in polymeric matrices is feasible. However, rather high nickel loadings and magnetic fields may be necessary to achieve economical fiber rotation rates.

To study saturation effects on magnetic torque, stonger magnetic fields have to be produced. This requires a more powerful magnet system than was available for the present study. Furthermore, particle interactions and the influence of particle aspect ratio on magnetic torque must be taken into consideration.

Several qualitative experiments conducted but not reported here indicated that, at reduced fluid viscosities, field strengths and magnetic loading levels can be reduced considerably and alignment still achieved in fractions of a second. Extrapolation to low fluid viscosities using the present equation of motion is limited because such equations for particle rotation in a low viscosity medium—such as air—must include the contribution of particle inertia. Furthermore, the hydrodynamic torque term must be changed to account for pressure drag. The magnetic torque and its dependencies discussed above do, however, remain unchanged. Both fiber alignment in low viscosity fluids and the issue of particle interactions offer promise for future study.

REFERENCES

BRENNER, H. 1963. The Stokes resistance to an arbitrary particle. Chem. Eng. Sci. 18(1):1–25.

BROWN, W. F. 1962. Magnetostatic principles in ferromagnetism. *In* E. P. Wohlfarth, ed. Selected topics in solid state physics, vol. I. North-Holland Publ. Co., Amsterdam, The Netherlands, and Interscience Publishers, New York, NY.

GREEN, H. V., T. J. FOX, AND A. M. SCALLAN. 1982. Lumen-loaded paper pulp. Pulp Pap. Can. 83(7):39–43.

HAPPEL, J., AND H. BRENNER. 1965. Low Reynolds number hydrodynamics with special applications to particulate media. Prentice Hall, Englewood Cliffs, NJ.

HATTA, H., AND S. YAMASHITA. 1988. Fiber orientation control by means of magnetic moment. J. Compos. Mater. 22:484–500.

HUMPHREY, P. E. 1995. Engineering composites from oriented natural fibres: A strategy. Pages 213–220 *in* J. F. Kennedy, G. O. Phillips, and P. A. Williams, eds. Chemistry and processing of wood and plant fibrous materials. Woodhead Publishing. Abingdon, UK.

JEFFERY, G. B. 1922. The motion of ellipsoidal particles immersed in a viscous fluid. Proc. R. Soc. London Ser. A 102(A715):161–179.

JOSEPH, R. I., AND E. SCHLÖMANN. 1965. Demagnetizing field in nonellipsoidal bodies. J. Appl. Phys. 36:1579–1593.

KAWAI, S., AND H. SASAKI. 1989. Oriented medium-density fiberboard produced with an eletrostatic field I. Mokuzai Gakkaishi 35:218–226.

————, ————, AND M. NORIMOTO. 1987. Aligning torque generated on wood particles by an electrostatic field I. Mokuzai Gakkaishi 33:872–878.

KELLY, A., AND G. J. DAVIES. 1965. The principles of fibre reinforcement of metals. Metall. Rev. 10(37):1–75.

KIM, S., AND S. J. KARRILA. 1991. Microhydrodynamics: Principles and applications. Butterworth-Heinemann, Boston, MA.

KLAUDITZ, W. VON, H. J. ULBRICHT, W. KRATZ, AND A. BURO. 1960. Herstellung und Eigenschaften von Holzpanwerkstoffen mit gerichter Festigkeit. Holz Roh-Werkst. 18:377–385.

KNOBLACH, G. M. 1989. Using electric fields to control fiber orientation during the manufacturing of composite materials. SAMPE J. 25(6):9–16.

———— 1990. Processing electric fields for fiber orientation. Pages 413–424 *in* S. M. Lee, ed. International encyclopedia of composites, vol. 4. VCH Publishers, New York, NY.

NAGASAWA, C., Y. KUMAGAI, AND K. URABE. 1990. Electromagnetic shielding effectiveness of particleboard containing nickel-metalized wood particles in the core layer. Mokuzai Gakkaishi 36:531–537.

————, ————, AND ————. 1991. Electroconductivity and electromagnetic shielding effectiveness of nickel-plated veneer. Mokuzai Gakkaishi 37:158–163.

————, ————, N. KOSHIZAKI, AND T. KANBE. 1992. Changes in electromagnetic shielding propert es of particleboards, made of nickel-plated wood particles formed by various pre-treatment processes. Mokuzai Gakkaishi 38:256–263.

NILAKANTAN, P. 1938. Magnetic anisotropy of naturally occurring substances. Proc. Indian Acad. Sci. Ser. A 7(1):38–49.

OKAGAWA, A., AND S. G. MASON. 1974. Particle behavior in shear and electric fields. VII. Orientation distributions of cylinders. J. Colloid Interface Sci. 47:568–587.

————, A. G. COX AND S. G. MASON. 1974. Particle behavior in shear and electric fields. VI. The microrheology of rigid spheroids. J. Colloid Interface Sci. 47:537–567.

PULIDO, O. R., S. KAWAI, Y. YOSHIDA, AND H. SASAKI. 1990. Oriented medium-density fiberboard produced

with an electrostatic field II. Mokuzai Gakkaishi 36:29–35.

———, H. SASAKI, S. KAWAI, AND Y. YOSHIDA. 1991a. Oriented mat-former with high voltage electrode system II. Mokuzai Gakkaishi 37:1167–1176.

———, Y. YOSHIDA, S. KAWAI, AND H. SASAKI. 1991b. Aligning torque generated in wood particles by an electrostatic field IV. Mokuzai Gakkaishi 37:135–141.

———, ———, Q. WANG, S. KAWAI AND H. SASAKI. 1991c. Aligning torque generated in wood particles by an electrostatic field V. Mokuzai Gakkaishi 37:711–718.

RICARD, S., AND R. H. MARCHESSAULT. 1990. Preparation of in situ magnetically loaded cellulose fibers. Pages 319–325 in Materials Research Society Symposium Proceedings, vol. 197. Materials Research Society, Pittsburgh, PA.

RIOUX, P., S. RICARD, AND R. H. MARCHESSAULT. 1992. The preparation of magnetic papermaking fibres. J. Pulp Pap. Sci. 18(1):J39–J43.

SCHLESINGER, M. 1974. The basic principles of electroless deposition. Pages 176–182 in B. N. Chapman and J. C. Anderson, eds. Science and technology of surface coating. Academic Press, London, UK, and Academic Press, New York, NY.

SCHWARTZ, M., AND G. O. MALLORY. 1976. Effect of heat-treatments on magnetic properties of electroless nickel alloys. J. Electrochem. Soc. 123:606–614.

SHINE, A. D. 1982. The rotation of suspended ferromagnetic fibers in a magnetic field. Ph.D. thesis, Massachusetts Institute of Technology, Cambridge, MA.

SIEMENS, AG. 1979. The vacuumschmelze handbook. Soft magnetic materials: Fundamentals, alloys, properties, products, applications. R. Boll, ed. Siemens AG, Berlin and Munchen, Germany, and Heyden & Son Ltd. London, UK.

STRATTON, J. A. 1941. Electromagnetic theory. McGraw-Hill Book Co., Inc., New York, NY.

SUCHSLAND, O., AND G. E. WOODSON. 1987. Fiberboard manufacturing practices in the United States. USDA Forest Serv. Agric. Handb. No. 640, Washington, DC.

SUTTON, W. H. 1970. Principles and methods for fabricating whisker-reinforced composites. Pages 273–342 in A. P. Levitt, ed. Whisker technology. Wiley Interscience, New York, NY.

TALBOTT, J. W. 1974. Electrically aligned particleboard and fiberboard. Pages 153–182 in T. M. Maloney, ed. Proc. 8th Particleboard Symposium. Washington State Univ., Pullman, WA.

———, AND E. K. STEFANAKOS. 1972. Aligning forces on wood particles in an electric field. Wood Fiber Sci. 4:193–203.

YAMASHITA, S., H. HATTA, T. SUGANO, AND K. MURAYAMA. 1989. Fiber orientation control of short fiber composites experiment. J. Compos. Mater. 23(1):32–41.

YOSHIDA, Y., S. KAWAI, O. R. PULIDO, AND H. SASAKI. 1989. Production of oriented particleboard I. Mokuzai Gakkaishi 35:227–233.

———, O. R. PULIDO, S. KAWAI, AND H. SASAKI. 1988. Aligning torque generated in wood particles by an electrostatic field II. Mokuzai Gakkaishi 34:401–408.

———, ———, ———, AND ———. 1990. Aligning torque generated on wood particles by an electrostatic field III. Mokuzai Gakkaishi 36: 523–530.

ZAUSCHER, S. 1992. Orienting lignocellulosic fibers by means of a magnetic field. M.S. thesis, Oregon State University, Corvallis, OR.

———. 1993. Orientation of lignocellulosic fibers in liquid systems by means of an electric field. An experimental approach. Unpublished report for the USDA Forest Products Lab., Madison, WI.